

Radiative corrections to W , Z masses and constraints on new Z bosons

V. Barger and J. L. Hewett

Physics Department, University of Wisconsin, Madison, Wisconsin 53706

T. G. Rizzo

Physics Department, University of Wisconsin, Madison, Wisconsin 53706

and Ames Laboratory and Physics Department, Iowa State University, Ames, Iowa 50011

(Received 3 April 1990)

We explore the implications of the recent W - and Z -boson-mass measurements at the SLAC Linear Collider, CERN LEP, and Fermilab Tevatron, and also the μ pair and total hadronic cross sections measured at KEK TRISTAN. A detailed comparison is made between the M_W and M_Z data and standard-model predictions including radiative corrections. These measurements also constrain extended electroweak gauge models. We place model-dependent upper bounds on the mass of a second neutral gauge boson from M_W and M_Z data, and set lower bounds on the Z' mass from direct production searches at the Collider Detector at Fermilab (CDF). We analyze the effects of Z - Z' mixing on the Z width, leptonic branching ratio, and peak cross section at e^+e^- colliders. We find that a second Z cannot account for the increase in total hadronic and decrease in μ -pair cross sections observed at KEK TRISTAN and simultaneously satisfy the CDF Z' search limits.

I. INTRODUCTION

Once the masses and widths of the W and Z gauge bosons are accurately determined, further precision tests of the standard model (SM) can be made. Until lately these masses were experimentally measured only at the level of 1–2% and the W and Z widths were not well determined.¹ The new measurements² of M_Z by the Mark II Collaboration ($M_Z=91.14\pm 0.12$ GeV) at the SLAC Linear Collider (SLC) and the ALEPH, DELPHI, L3, and OPAL Collaborations at CERN LEP (with a combined result $M_Z=91.155\pm 0.033$ GeV) as well as the Collider Detector at Fermilab (CDF) Collaboration measurement³ of M_W at the Fermilab Tevatron ($M_W=80.0\pm 0.4\pm 0.2$ GeV) have now provided us with a new proving ground for the SM. In addition, CDF reports a preliminary measurement of the mass difference $M_Z-M_W=10.9\pm 0.5$ GeV. The number of neutrinos (N_ν) extracted from the height of the Z peak as well as a measurement of the width of the Z itself have been obtained at both the SLC and LEP. A combined fit to the LEP data yields $N_\nu=3.16\pm 0.11$ and $\Gamma_Z=2.546\pm 0.031$ GeV. This set of measurements, as well as recent results from KEK TRISTAN,⁴ can be used to severely constrain new physics beyond the SM.

In Sec. II, we make a comparison with recently measured values of M_Z , M_W , and Γ_Z , with the radiatively corrected SM. The SM agrees with the new data, but the errors in the data are still large enough to allow for some deviation from the SM, such as that which may occur in alternative electroweak gauge models.

In Sec. III we examine how the mixing of the SM Z with a second neutral gauge boson, Z' in several classes of extended electroweak models would influence a number of Z -boson properties, i.e., its leptonic branching

fraction, full width, and the height of the resonance peak at e^+e^- colliders. We find that the latter quantity is particularly sensitive to Z - Z' mixing for the models examined. Further, using the CDF, LEP, and Mark II data on the W and Z masses, we obtain model-dependent upper limits on the mass of the Z' and compare these with the preliminary lower limits on these masses from the direct search by CDF.

In Sec. IV we explore the possibility that the deviations from the SM predictions for the cross sections for μ -pair and hadron production in e^+e^- annihilation observed at KEK TRISTAN may be the result of the existence of a new Z' gauge boson. For the set of models examined, we will show that the contributions of a Z' satisfying the CDF preliminary search limits are much too small to explain the size of either effect.

Our summary and conclusions can be found in Sec. V.

II. STANDARD-MODEL ANALYSIS

The radiative corrections to M_W and M_Z are well understood within the context of the SM. In the on-shell renormalization scheme of Marciano and Sirlin⁵ the weak mixing angle $\sin^2\theta_W$ ($\equiv x_W$) is defined via

$$x_W = 1 - M_W^2/M_Z^2 \quad (2.1)$$

and the radiatively corrected Z mass can be expressed as

$$M_Z^2 = \frac{A}{x_W(1-x_W)(1-\Delta r)}, \quad (2.2)$$

where $A \equiv \pi\alpha(m_e)/\sqrt{2}G_F \simeq (37.28022 \text{ GeV})^2$ for $\alpha^{-1}(m_e)=137.0359895$ and $G_F=1.166389 \times 10^{-5} \text{ GeV}^{-2}$. The effects of the radiative corrections are contained in Δr which depends on M_Z and the masses of the top quark (m_t) and Higgs boson (m_H). For given values

of m_t and m_H , the values of the x_W and Δr are extracted in our analysis from the experimental value of M_Z by the following procedure. (i) We first determine x_W and Δr at the one-loop level from the program of Halzen and Morris⁶ which uses the exact expressions given by Hollik.⁷ We denote these values by x_W^1 and Δr_1 . (ii) We then include the leading two-loop contributions to Δr . These consist of the QCD corrections to the usual top-quark loop⁸ which are given by

$$\Delta r_2^{\text{QCD}} \simeq \frac{1-x_W}{x_W} \left[\frac{3G_F m_t^2}{8\sqrt{2}\pi^2} \right] \left[\frac{2\pi^2+6}{9} \right] \frac{\bar{\alpha}_s}{\pi}, \quad (2.3)$$

where $\bar{\alpha}_s$ is the value of α_s evaluated at scale $m_t + m_b$, and the two-loop quark contribution⁹ which is given by

$$\Delta r_2^{\text{top}} \simeq \frac{1}{3}(2\pi^2-19) \left[\frac{3G_F m_t^2}{8\sqrt{2}\pi^2} \right]^2 \left[\frac{1-x_W}{x_W} \right]. \quad (2.4)$$

We evaluate these two contributions with $x_W = x_W^1$ and add them to Δr_1 . (iii) Including the above one- and two-loop contributions to Δr , we use Eq. (2.2) to determine a two-loop corrected value of x_W . (iv) We iterate the solution until the values of x_W and Δr converge. Our final results are identical to those given by Hollik⁷ (at the level of 1 part in 10^4) over the entire range of top-quark and Higgs-boson masses of interest and including the $O(\alpha^2)$ corrections.

Having determined x_W as a function of m_t and m_H for a given M_Z we proceed to calculate the width of the Z boson. We make use of the ‘‘improved born approximation’’ (IBA) discussed in Ref. 7, wherein the vector couplings of all the fermions are determined by an ‘‘effective’’ weak mixing angle \bar{x}_W obtained from x_W through the relation^{7,10,11}

$$\bar{x}_W = x_W + (1-x_W)\delta\rho_t + \frac{\alpha}{4\pi} \left[\ln \left[\frac{m_H}{17.3} + 1 \right] - 2 \right], \quad (2.5)$$

where

$$\delta\rho_t \simeq \frac{3G_F m_t^2}{8\sqrt{2}\pi^2} \left[1 - \frac{2\pi^2+6}{9} \frac{\bar{\alpha}_s}{\pi} + \frac{19-2\pi^2}{3} \left[\frac{3G_F m_t^2}{8\sqrt{2}\pi^2} \right] \right]. \quad (2.6)$$

The partial width can be written as

$$\Gamma(Z \rightarrow f\bar{f}) = (\Gamma_0)_f \left[\frac{1}{2}\beta_f(3-\beta_f^2)\bar{v}_f^2 + \beta_f^3\bar{a}_f^2 \right], \quad (2.7)$$

where $\beta_f = (1-4m_f^2/M_Z^2)^{1/2}$ is the velocity of the final-state fermions. The total width Γ_Z is obtained by summing over all fermion channels. The overall scale is given by

$$\Gamma_0 = N_c \frac{G_F M_Z^3}{6\sqrt{2}\pi} (1-\delta\rho_t)^{-1} \left[1 + \frac{3\alpha}{4\pi} Q_f^2 \right]. \quad (2.8)$$

Here $N_c = 1$ (3) for leptons (quarks) and Q_f is the electric charge of the fermion in the final state. In the case of $Z \rightarrow b\bar{b}$ the large t -quark vertex correction must be ac-

counted for by a further shift in the ‘‘effective’’ \bar{x}_W in the vector coupling of the b quark,

$$\bar{x}_W \rightarrow (\bar{x}_W)_b = \bar{x}_W(1+2\delta\rho_t/3), \quad (2.9a)$$

and a corresponding shift in the partial-width normalization^{7,10,11}

$$\Gamma_0 \rightarrow (\Gamma_0)_b = \Gamma_0(1-4\delta\rho_t/3). \quad (2.9b)$$

For hadronic final states, QCD corrections are also included by rescaling the vector and axial-vector coupling constants of the quarks:

$$v_q^2 \rightarrow v_q^2 \left[1 + c_1 \left[\frac{\alpha_s}{\pi} \right] + c_2 \left[\frac{\alpha_s}{\pi} \right]^2 + c_3 \left[\frac{\alpha_s}{\pi} \right]^3 \right] \equiv \bar{v}_q^2, \quad (2.10)$$

$$a_q^2 \rightarrow a_q^2 \left[1 + d_1 \left[\frac{\alpha_s}{\pi} \right] + d_2 \left[\frac{\alpha_s}{\pi} \right]^2 + d_3 \left[\frac{\alpha_s}{\pi} \right]^3 \right] \equiv \bar{a}_q^2,$$

where the couplings are normalized such that $a_u = +\frac{1}{2}$. The coefficients c_{iq} and d_{iq} are given in Refs. 10 and 12. Note that we include the leading finite m_b^2/M_Z^2 corrections in c_1 and d_1 as well as the sizable m_t -dependent corrections in d_{2q} .¹² The charm-quark and τ -lepton masses are also retained in our calculations; we use the values $\alpha_s(M_Z^2) = 0.12$, $m_b = 5$ GeV, $m_c = 1.5$ GeV, and $m_\tau = 1.784$ GeV.

Figure 1 shows the prediction for Γ_Z as a function of m_t , with $m_H = 10, 100,$ and 1000 GeV for $M_Z \pm 1\sigma$, assuming $N_\nu = 3$. Note that for $m_t = m_H = 100$ GeV we find $\Gamma_Z = 2.489$ GeV which is about 2σ below the central value of Γ_Z from the LEP data. For the W -boson width, assuming $m_t + m_b > M_W$ and taking the central values of Kobayashi-Maskawa matrix elements given by Ref. 13 we obtain $\Gamma_W = 2.06 \pm 0.04$ GeV, where the error reflects the experimental uncertainty in the W mass. Present data¹⁴ from CDF are consistent with this value of Γ_W .

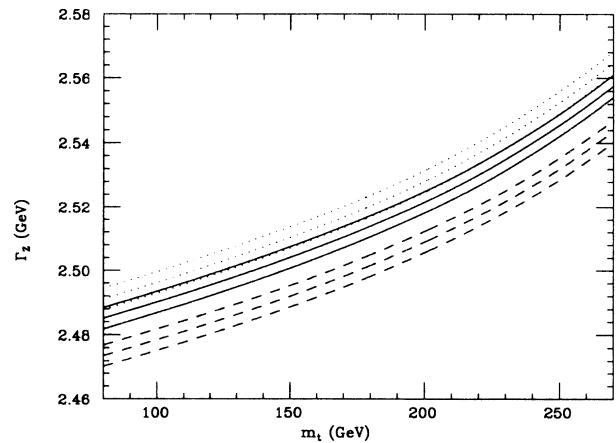


FIG. 1. The Z -boson width (Γ_Z) as a function of the top-quark mass (m_t) for different values of m_H including electroweak and QCD corrections and assuming $m_b = 5$ GeV, $N_\nu = 3$, and $\alpha_s = 0.12$ as described in the text. The dotted (solid, dashed) curve corresponds to $m_H = 10$ (100, 1000) GeV.

We next calculate the value of M_Z which results from using the CDF measurement of M_W ($=80.0 \pm 0.45$ GeV) as input. For a given M_W we calculate x_W for a set of values of m_t and m_H . The value of x_W extracted in this manner is shown in Fig. 2(a). Using the relation $M_Z = M_W / (1 - x_W)$ we then obtain M_Z as a function of m_t , as shown in Fig. 2(b). Note that $M_W = 79.55$ GeV leads to values of M_Z which are significantly more than 1σ outside the range of the LEP data, while for $M_W = 80.45$ GeV, m_t must lie in the range $170 \leq m_t \leq 210$ GeV in order to obtain agreement with the LEP data. Thus at the 1σ level we must have $m_t \lesssim 210$ GeV for consistency with the Z mass determination. Our values of x_W extracted from M_W are in good agreement with those obtained by Ellis and Fogli,¹⁵ $x_W = 0.2284^{+0.0046+0.0029}_{-0.0032-0.0025}$, from low-energy neutral-current data¹⁶ with radiative corrections included. In their x_W determination the

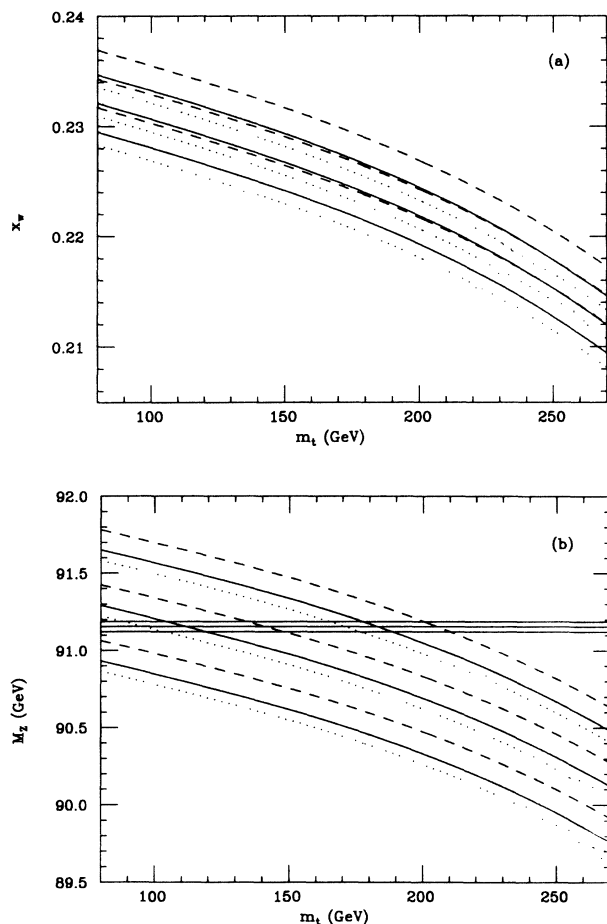


FIG. 2. (a) x_W extracted from the value of M_W as functions of m_t with $m_H = 10$ GeV (dotted), 100 GeV (solid), or 1000 GeV (dashed). The upper (middle, lower) curve in each case corresponds to $M_W = 79.55$ (80.0, 80.45) GeV and reflects the errors in the mass measurements. (b) M_Z as a function of m_t using the values of x_W in (a) and the values of M_W from CDF for different values of the Higgs-boson mass as denoted in (a). The upper (middle, lower) curves correspond to $M_W = 80.45$ (80.0, 79.55) GeV.

above uncertainties are experimental and theoretical, respectively, and all values of m_t are considered in the uncertainties. An improvement in the measurement of M_W at the level of $\Delta M_W = \pm(0.1-0.3)$ GeV would be extremely useful in testing the SM by reducing the allowed ranges of both x_W and M_Z for given values of m_t and m_H . In the next Fermilab Tevatron Collider run, it is expected that CDF will reduce the uncertainty on their measurement of M_W to $\Delta M_W = 0.3-0.4$ GeV.³

A further test of the SM can be made when the W and Z mass splitting, $M_Z - M_W$ is accurately determined. The combined CDF, SLC, and LEP data indicate^{2,3} that this splitting lies in the rather broad range $10.4 \leq M_Z - M_W \leq 11.4$ GeV at the 1σ level. Figure 3(a) shows $M_Z - M_W$ as a function of M_Z as well as the 1σ al-

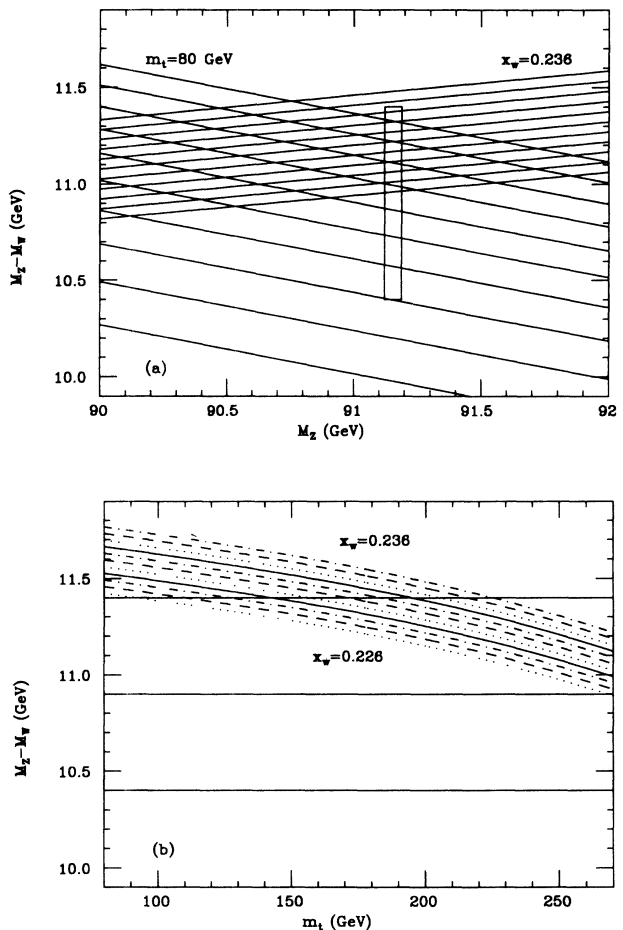


FIG. 3. $M_Z - M_W$ as a function of (a) M_Z and (b) m_t . In (a), the curves with positive slope show the variation with x_W decreasing in steps of 0.001 starting with $x_W = 0.236$ which yields the largest value of $M_Z - M_W$. The curves with negative slope show, for $m_H = 100$ GeV, the m_t dependence of $M_Z - M_W$ for $80 \leq m_t \leq 260$ GeV in steps of 20 GeV with $m_t = 260$ GeV giving the smallest value of $M_Z - M_W$. In (b), the highest (lowest) curve corresponds to $x_W = 0.236$ (0.226) and decreases in steps of 0.001. Here $m_H = 100$ GeV is assumed. Present bounds from CDF and LEP are also shown.

lowed regions on M_Z (from LEP) and on $M_Z - M_W$. There is a twofold relationship between $M_Z - M_W$ and M_Z as follows. In the on-shell scheme $M_W = M_Z \cos\theta_W$, and thus

$$M_Z - M_W = M_Z(1 - \cos\theta_W), \quad (2.11)$$

independent of the values of m_t, m_H , etc. On the other hand, one can extract x_W from M_Z (for a given set of m_t and m_H values), then calculate M_W , and subsequently determine $M_Z - M_W$; this gives $M_Z - M_W$ as a function of M_Z in a manner which depends on m_t and m_H . In Fig. 3(a) the curves with positive slope correspond to the relationship (2.11) for different choices of x_W and are m_t and m_H independent, whereas those with negative slope are obtained from the second method (with $m_H = 100$ GeV) and correspond to different values of m_t . For $m_H = 10$ (1000) GeV the predicted values of $M_Z - M_W$, for a fixed value of M_Z , shift downward (upward) by an amount $\simeq 80$ – 90 (170–180) MeV. Unfortunately the slopes of both sets of curves are small in magnitude and hence further refinements in the mass splitting measurement will be necessary before certain values of m_t and x_W can be excluded by this data. Unlike separate measurements of M_W and M_Z , the splitting $M_Z - M_W$ should suffer less from experimental systematic uncertainties so that eventually one may expect a reasonably small overall error on the difference.

Instead of displaying $M_Z - M_W$ as a function of M_Z , the explicit dependence of $M_Z - M_W$ on m_t can be determined (for a fixed m_H and given values of x_W) by using the equations above. This result is shown in Fig. 3(b) for different choices of x_W with $m_H = 100$ GeV. $M_Z - M_W$ as a function of m_t is not very sensitive to variations of m_H , i.e., for $m_H = 10$ (1000) GeV the curves for a fixed value of m_t are only shifted downward (upward) by an amount $\simeq 20$ – 30 (50–70) MeV. Figure 3(b) also shows that for a given m_H and x_W , $M_Z - M_W$ is not especially sensitive to m_t and decreases by only $\simeq 0.55$ GeV as m_t increases from 80 to 270 GeV.

If new physics exists beyond that contained in the SM, one can examine its effects on the $M_Z - M_W$ mass splitting. The relationships between $M_Z - M_W$ and any new model parameters will in general be quite complicated and difficult to analyze. However, in a certain class of models $M_Z - M_W$ can be directly related to Δr . Consider the class of models based on $SU(2)_L \times U(1)_Y$ with only Higgs doublets and singlets so that the relationship $M_Z = M_W / \cos\theta_W$ is maintained naturally. In these models for a given value of Δr and using the M_Z measurement from LEP we can calculate $M_Z - M_W$ by combining Eqs. (2.1) and (2.2). Defining $\delta = M_Z - M_W$, we obtain

$$\Delta r = 1 - \frac{A / (M_Z - \delta)^2}{1 - (M_Z - \delta)^2 / M_Z^2}. \quad (2.12)$$

Figure 4 shows $M_Z - M_W$ as a function of Δr using the LEP measurements of M_Z ($\pm 2\sigma$). This result holds in all models without new gauge bosons and which contain only scalar fields which transform as singlets and doublets under $SU(2)_L$ including, e.g., the two-Higgs-doublet

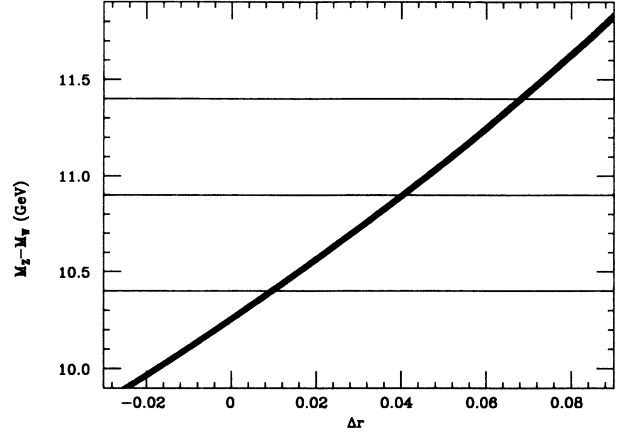


FIG. 4. $M_Z - M_W$ as a function of Δr corresponding to 2σ errors on M_Z from the combined LEP fit.

model and the minimal supersymmetric SM. The present 1σ bound on $M_Z - M_W$ from CDF ($= 10.9 \pm 0.5$ GeV) already restricts Δr to the range $0.01 \leq \Delta r \leq 0.07$; if, for example, it should be determined that $M_Z - M_W = 10.9 \pm 0.2$ GeV in the near future then we would obtain instead that $0.03 \leq \Delta r \leq 0.05$ which is a very substantial improvement and could be used to pin down new physics beyond that contained in the SM. Note that the relationship (2.12) is exact to all orders since it follows directly from the definitions in (2.1) and (2.2).

III. MODELS WITH NEW NEUTRAL GAUGE BOSONS

In this section we will focus on the implications of existing (and near future) e^+e^- and hadron collider measurements of the properties of the W and Z on models where the electroweak gauge group contains at least an additional $U(1)$ factor, i.e., at least one new neutral gauge boson exists. As is well known, the mixing of the SM Z with a heavier Z' naturally leads to a decrease in the observed mass (M_1) of the lighter neutral gauge boson (Z_1) so that there will be a strong interplay between effects from radiative corrections and those from mixing.

To be concrete we focus our attention on three specific extended electroweak models: the class of E_6 superstring-inspired models¹⁷ of the effective rank-5 type (ER5M), the superstring-inspired alternative to the usual left-right-symmetric model^{17,18} (ALRM), and the classic left-right-symmetric model (LRM) itself.¹⁹ We note that in the ER5M and ALRM the Higgs fields transform only as $SU(2)_L$ doublets and singlets. The ER5M contains an additional mixing angle θ which affects the couplings of the Z' in these models and originates from the breaking pattern

$$\begin{aligned} E_6 &\rightarrow SO(10) \times U(1)_\psi \rightarrow SU(5) \times U(1)_\chi \times U(1)_\psi \\ &\rightarrow SM \times U(1)_\theta \end{aligned} \quad (3.1)$$

with $Z'(\theta) = Z_\psi \cos\theta - Z_\chi \sin\theta$ being the additional ‘‘light’’ gauge boson. Apart from θ , all of the couplings

of the Z' are completely fixed by the group theory of E_6 and are given by the Lagrangian ($c = \cos\theta_W$)

$$\mathcal{L} = \frac{g}{c}(T_3 - x_W Q)Z + \frac{g}{c} \left[\frac{5x_W}{3} \right]^{1/2} (Q_\psi \cos\theta - Q_\chi \sin\theta)Z'. \quad (3.2)$$

Here Q is the ordinary electric charge, $T_3 = T_{3L} + T_{3R}$, and $Q_{\psi,\chi}$ simply relate¹⁷ how a given field transforms under $U(1)_{\psi,\chi}$. Explicit models discussed in the literature correspond to particular values of θ : model ψ ($\theta=0^\circ$), model χ ($\theta=-90^\circ$), and model η ($\theta=\arccos\sqrt{5/8} \simeq 37.76^\circ$) will be considered in our analysis below.

In both the LRM and the ALRM, the left-handed [right-handed fermions] transform as doublets under $SU(2)_L$ [$SU(2)_R$] and the symmetries are broken by a mixed doublet Higgs representation together with a Higgs doublet (LRM or ALRM) or triplet (LRM only) under $SU(2)_L$ and $SU(2)_R$. In the case of the Higgs triplets in the LRM, the left-handed triplet vacuum expectation value (VEV) can be chosen to be vanishingly small, while the right-handed Higgs fields always transform as an $SU(2)_L$ singlet in either case. The ALRM makes use of a fermion assignment ambiguity within the **27** representation of E_6 and interchanges the quantum numbers of some of the ordinary and E_6 exotic fermions. This forces the gauge boson W_R to couple the ordinary fermions to the exotic fermion fields and carry both lepton number and negative R parity. In both the ALRM and LRM, the couplings are given by the Lagrangian

$$\mathcal{L} = \frac{g}{c}(T_3 - x_W Q)Z + \frac{g}{c}(1 - 2x_W)^{-1/2} [x_W T_{3L} + (1 - x_W)T_{3R} - x_W Q]Z', \quad (3.3)$$

but the quantum number assignments of the fermions and Higgs fields are quite distinct in these two models.

In all of the above models, the Z - Z' mass matrix takes the form

$$\mathcal{M}^2 = \begin{pmatrix} M_Z^2 & \delta M^2 \\ \delta M^2 & M_Z'^2 \end{pmatrix} \quad (3.4)$$

with $M_Z^2 = M_W^2/c^2$, even when radiative corrections are included, since the only Higgs fields with nonzero VEV's are doublets and singlets. Strictly speaking, this is true in the LRM only if the W does not mix with the W_R ; however, since M_{W_R} is constrained to be $\gtrsim 2$ TeV in this model, one expects W - W_R mixing to be quite small.^{19,20} In the ALRM, W and W_R are forbidden to mix because of R -parity conservation.

In the ER5M and ALRM, δM^2 is given by

$$\delta M^2/M_Z^2 = 2(Q'_1 \cos^2\beta - Q'_2 \sin^2\beta), \quad (3.5)$$

where $\tan\beta \equiv v_2/v_1$ is the ratio of the two Higgs-doublet VEV's in these models and

$$Q'_1 = \left[\frac{5x_W}{3} \right]^{1/2} \left[-\frac{1}{\sqrt{6}} \cos\theta + \frac{1}{\sqrt{10}} \sin\theta \right], \quad (3.6)$$

$$Q'_2 = \left[\frac{5x_W}{3} \right]^{1/2} \left[-\frac{1}{\sqrt{6}} \cos\theta - \frac{1}{\sqrt{10}} \sin\theta \right]$$

for the ER5M and

$$Q'_1 = \frac{1}{2}x_W(1 - 2x_W)^{-1/2}, \quad (3.7)$$

$$Q'_2 = \frac{1}{2}(1 - 2x_W)^{1/2}$$

in the ALRM. In the LRM, δM^2 is given by

$$\delta M^2/M_Z^2 = -(1 - 2x_W)^{1/2}. \quad (3.8)$$

Diagonalization of the mass matrix in Eq. (3.4) via the rotation

$$\begin{pmatrix} Z_1 \\ Z_2 \end{pmatrix} = \begin{pmatrix} \cos\phi & \sin\phi \\ -\sin\phi & \cos\phi \end{pmatrix} \begin{pmatrix} Z \\ Z' \end{pmatrix} \quad (3.9)$$

leads to mass eigenstates $Z_{1,2}$ with mass $M_{1,2}$ ($M_1 < M_2$) and the relations

$$\tan^2\phi = \frac{M_Z^2 - M_1^2}{M_2^2 - M_Z^2}, \quad (3.10)$$

$$\frac{\delta M^2}{M_Z^2} = - \left[\frac{M_2^2}{M_Z^2} - 1 \right] \tan\phi.$$

Z - Z' mixing not only produces a shift in the mass of the Z but there is also an induced change in its couplings which may be probed by making detailed analyses at the Z_1 resonance. Letting $\lambda(\lambda')$ represent a generic Z (Z') coupling, mixing between the Z and Z' produces the Z_1 couplings $\lambda_1 = \lambda \cos\phi + \lambda' \sin\phi$, where ϕ is defined above in Eq. (3.9). This change in the couplings modifies, e.g., the value of Γ_Z , the height of the visible cross-section peak (σ), and the leptonic branching fraction B . Figure 5(a) shows the variation of the total Z width in percent in the ER5M for all values of θ and for $-0.15 \leq \phi \leq 0.15$ which encompasses all of its allowed range.¹³ (However, as we will see, the preliminary limits on M_2 from CDF indicate that $|\phi| \leq 0.05$). We have taken $M_1 = 91.155$ GeV and $\alpha_s = 0.12$ in this analysis. One sees that it is relatively easy to decrease Γ_Z by a few percent via Z - Z' mixing but somewhat harder to increase Γ_Z by this mechanism (an increase of +5.0% is obtained only for $|\phi| > 0.15$). Figure 5(b) shows $\Gamma_Z/\Gamma_Z^{\text{SM}}$ as a function of ϕ for both the LRM and ALRM; one sees that changes in Γ_Z of a few percent at most are possible for this range of mixing angle. Note that in terms of N_ν , a 3.3% change in Γ_Z corresponds to $\Delta N_\nu \simeq \frac{1}{2}$. The central value for the fitted width of the Z boson obtained at LEP ($\Gamma_Z = 2.546 \pm 0.031$ GeV), although somewhat larger than the SM prediction, can be obtained via Z - Z' mixing especially if m_t is large. The further accumulation of data at the SLC and LEP should clarify the width question in a few months time.

Figure 6(a) shows the percentage change in the Z leptonic branching fraction, B , due to mixing in the ER5M.

Notice that a much larger fraction of the parameter space leads to significant variations in B and only a small region allows for absolute values of changes in B less than 1%. This high sensitivity to Z - Z' mixing results from the small SM value of the electron vector coupling to the SM Z for x_W near $\frac{1}{4}$. Figure 6(b) shows B/B_{SM} for both the LRM and ALRM and that variations of order 5–10% are easily obtained for reasonable values of ϕ . The present combined statistical and systematic errors on B (≈ 40 –50%) are still too large to allow for a comparison with the SM, but further data from LEP should provide a good measurement by the end of 1990.

Since the peak cross section (together with the value x_W obtained from M_Z) is used to determine N_ν , it is also important to explore how this cross section might be modified by mixing. The cross section at the resonance peak is directly related to the leptonic width B and the branching fraction into all observable modes (i.e., e 's, μ 's, τ 's, and hadrons) and might therefore be even more sensitive to Z - Z' mixing than either B or Γ_Z . Figure 7(a) shows the change in the peak cross section (σ) in the

ER5M as a function of θ for $-0.15 \leq \phi \leq 0.15$. Comparing Fig. 7(a) with both Figs. 5(a) and 6(a), we see that σ is the most sensitive quantity (for almost all θ values) of Γ_Z , B , and σ to nonzero Z - Z' mixing. This same sensitivity to $\phi \neq 0$ shown by σ is displayed in Fig. 7(b) for both the LRM and ALRM; even modest values of ϕ lead to appreciable changes in the peak cross section. Once σ is accurately measured (and radiative corrections are accounted for), it will clearly be a good probe of Z - Z' mixing.

Combining the Higgs constraint of Eq. (3.5) with Eq. (3.10) we have the condition in the ER5M or ALRM cases that²¹

$$2Q'_{\min} \leq \pm \left[\frac{(M_Z^2 - M_1^2)(M_2^2 - M_Z^2)}{M_Z^4} \right]^{1/2} \leq 2Q'_{\max} \quad (3.11)$$

with Q'_{\min} (Q'_{\max}) being the smallest (largest) of $-Q'_1$ and Q'_2 . With either choice of sign in Eq. (3.11), an upper bound on M_2 is obtained if the measured M_1 is different than the SM prediction for M_Z . The theoretical value of M_Z depends on m_t and m_H and for some possible values

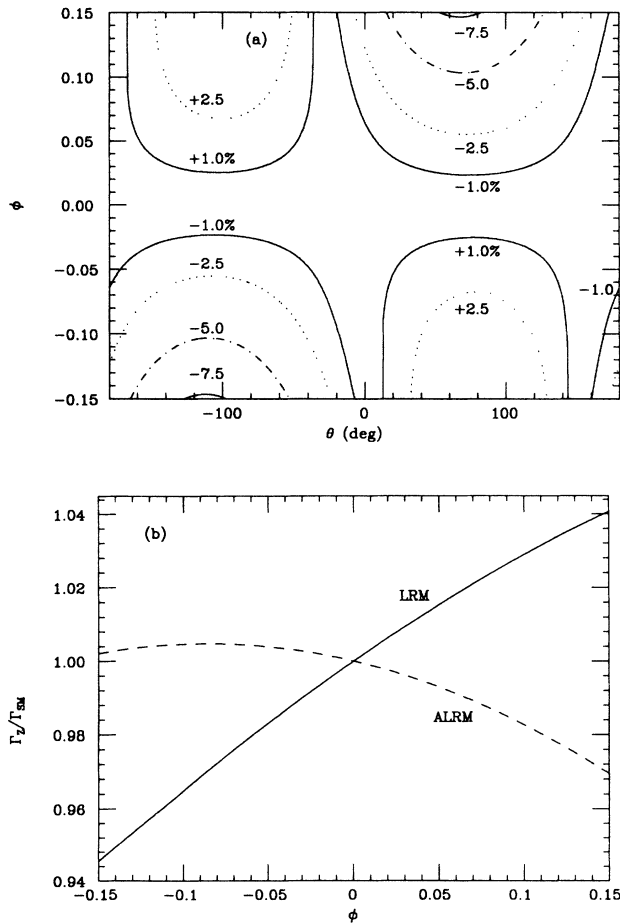


FIG. 5. Variations in the value of Γ_Z due to Z - Z' mixing. (a) Percentage changes in Γ_Z as a function of θ and ϕ for the ER5M assuming $M_1 = 91.155$ GeV and $\alpha_s = 0.12$. (b) the ratio of Γ_Z to its SM value as a function of ϕ for the LRM and ALRM with the same values of M_1 , x_W , and α_s as in (a).

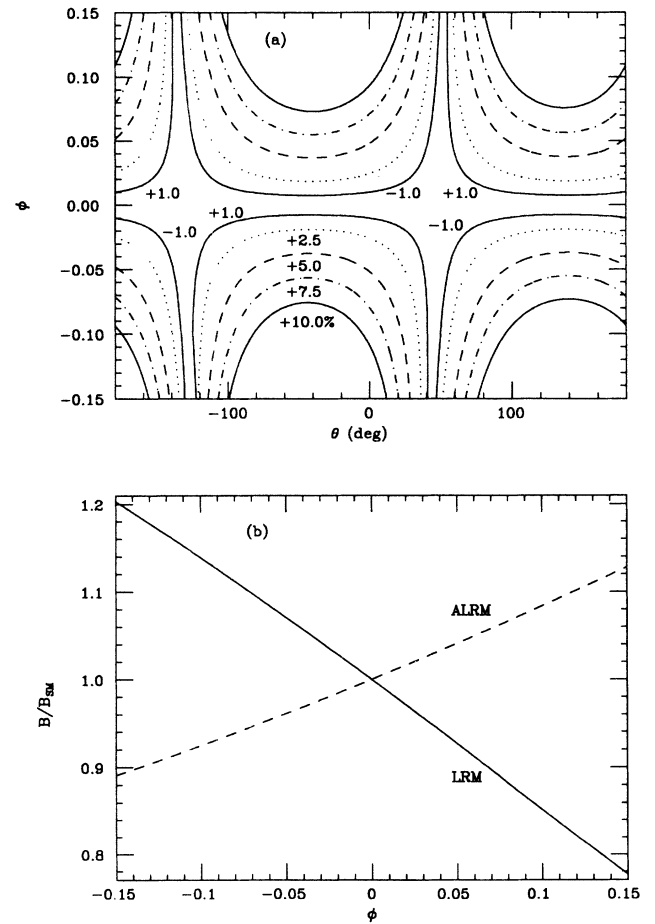


FIG. 6. Variations in the Z_1 leptonic branching fraction (B) due to Z - Z' mixing. (a) Percentage changes in B as a function of θ and ϕ for the ER5M using the same input as in Fig. 5 and using the same notation as in Fig. 5. (b) The ratio of B to its SM value as a function of ϕ for the LRM and ALRM.

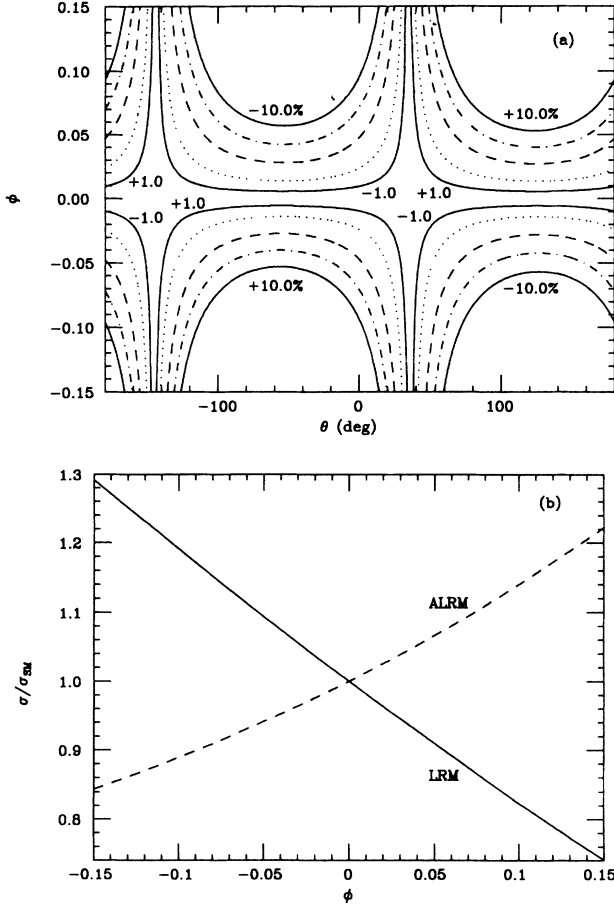


FIG. 7. Variations in the resonance peak cross section (σ) due to Z - Z' mixing. (a) Percentage change in σ as a function of θ and ϕ for the ER5M using the same input as in Fig. 5 and using the same notation as in Fig. 5. (b) The ratio of σ to its SM value as a function of ϕ for the LRM and ALRM.

of m_t and m_H , the theoretical M_Z agrees with the experimental M_1 ; then $\phi=0$ and Eq. (3.11) gives no restriction on M_2 . However for broad ranges of possible m_t, m_H values, the predicted M_Z is not consistent with the measured M_1 and then upper bounds on M_2 result from Eq. (3.11) assuming that Z - Z' mixing is the sole source of the Z_1 mass shift. A lower bound on M_2 is also obtained in the ER5M case from Eq. (3.11) for values of $\theta \geq \arccos(\sqrt{3}/8) \simeq 52.24^\circ$. In the LRM, one finds instead that M_2 is completely determined once M_Z and M_1 are known:

$$M_2 = M_Z \left[1 + \frac{(1 - 2x_W)M_Z^2}{M_Z^2 - M_1^2} \right]^{1/2}. \quad (3.12)$$

These results will be of critical importance in our analysis below.

From Eqs. (3.2) to (3.12) we can obtain an upper limit on M_2 in a model-dependent way, using the experimental value of M_1 and the expected value of M_Z in the SM. Note that here we cannot use M_1 to calculate x_W since it

is shifted from M_Z by Z - Z' mixing, but perhaps the other parameters in these equations may be useful. First, since the W mass and couplings are unaffected (at the tree level) by the existence of a Z' , we can use M_W to extract the value of x_W for a given value of m_t and m_H . This result is shown in Fig. 2(a). Note that in extended electroweak models m_H is now strictly just a parameter representing the combined scalar contributions to the radiative corrections for M_W . We then calculate M_Z^2 (the upper left-hand corner element of the Z - Z' mass matrix) via $M_Z^2 = M_W^2 / (1 - x_W)$. The resulting value of M_Z is shown in Fig. 2(b). This is the mass the SM Z would have if mixing with the Z' were absent. M_1 is then the physical mass of the lightest neutral boson, observed to be 91.155 ± 0.033 by LEP. M_Z is calculable, M_1 is measured, and by using x_W from M_W we can place upper bounds on M_2 (assuming $\phi \neq 0$) in both the ER5M and ALRM cases and calculate M_2 exactly in the LRM. These results will reflect the possible ranges of m_t and m_H values as well as the experimental uncertainties in both M_1 and M_W . Note that with Z - Z' mixing, smaller values of $M_1 - M_W$ become possible since M_1 is shifted downwards relative to M_Z by both radiative corrections and mixing while M_W is only modified via radiative effects.

The values of M_2 that we find from the analysis should be compared with the constraints from neutral-current data¹³ as well as the recent CDF preliminary search limits for new Z 's at the Fermilab Tevatron. Figure 8 shows the lower limit on M_2 obtained from the CDF preliminary²² result, $\sigma(p\bar{p} \rightarrow Z')B(Z' \rightarrow e^+e^-) \leq 1$ pb, as a function of the parameter θ in the ER5M for both the Duke and Owens²³ (DO I) and Eichten *et al.*²⁴ (EHLQ I) parton distribution functions. For θ outside the range in Fig. 8, the limit on M_2 is obtained by letting $\theta \rightarrow \theta + 180^\circ$ in the figure. In the LRM case, we find $M_2 \geq 363$ (355) GeV for DO I (EHLQ I) structure functions, while for

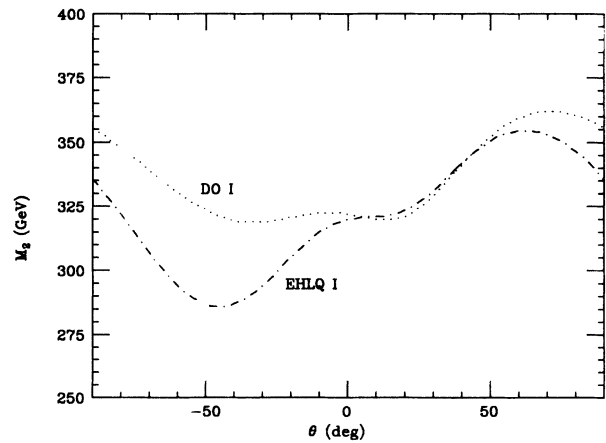


FIG. 8. Limits on the mass (M_2) of the Z_2 gauge boson as a function of θ in the ER5M from CDF assuming $\phi=0$ and using either Duke and Owens (DO I) or EHLQ I parton distribution functions.

the ALRM we find that $M_2 \geq 452$ (448) GeV for DO I (EHLQ I) structure functions. These bounds neglect Z - Z' mixing effects on the Z_2 couplings, assume $m_t = 90$ GeV, include a QCD enhancement factor²⁵ $K = 1 + 8\pi\alpha_s(\hat{s})/9$, and assume that the Z_2 decays only into the usual three generations of known fermions. It is quite important to notice that for the ER5M these limits show a strong dependency on the choice of distribution functions, in particular for values of θ near -50° ; this reflects the vanishing of the u -quark coupling to Z_2 for $\theta = -\arccos\sqrt{3/8} \approx -52.24^\circ$ and the relative size of the $d\bar{d}$ luminosity for the two sets of distribution functions. Neither the LRM nor the ALRM bounds show much sensitivity to the choice of parton distribution functions. We also note that the limits in the ER5M are weaker than those for either the LRM or the ALRM since the couplings are somewhat smaller in the ER5M case while those in the ALRM allow for a large leptonic branching ratio for the Z_2 . In the ALRM, the values of the Z' and the W_R masses are related (since they come from the

same VEV's) approximately by $M_2 \approx [(1-x_W)/(1-2x_W)]^{1/2} M_{W_R}$. The CDF Z' search limits then indirectly imply that $M_{W_R} > 378$ GeV. If we relax the assumption that $\phi=0$, how are these limits modified? A short analysis shows that for $|\phi| \lesssim 0.1$ these lower bounds are not altered by more than 5–10 GeV in either direction compared with the $\phi=0$ results. This shift is comparable to the uncertainty due to the choice of parton distribution functions.

In fact if the preliminary CDF Z' search limit is roughly correct, giving $M_2 \gtrsim 300$ GeV, then it is easy to show¹⁷ that $|\phi| \lesssim 0.05$ independent of the specific model under consideration if the shift in the Z mass due to Z - Z' mixing is at most 1 GeV. This follows immediately from the first relation in Eq. (3.10), given the experimental value of M_1 and the assumption that the difference $M_Z - M_1$ due to mixing is less than 1 GeV. Tighter limits on ϕ will apply in both the LRM and ALRM since we obtain even stronger lower bounds on M_2 in these models. Similar limits are obtained by constraints coming from the Higgs sector of these models.

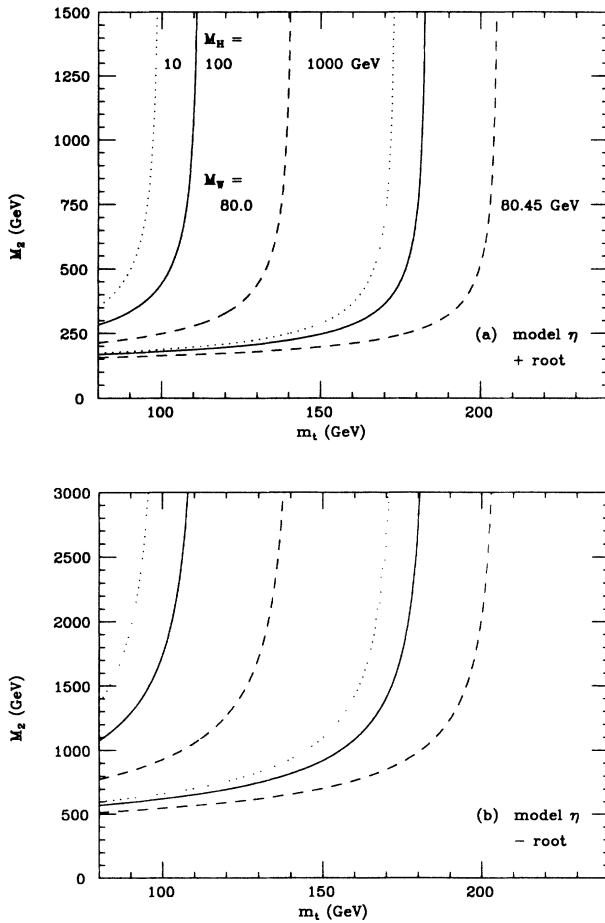


FIG. 9. Upper bound on M_2 as a function of m_t for model η assuming $m_H = 10$ (dotted), 100 (solid), and 1000 (dashed) GeV with $M_W = 80.0$ GeV (left curves) and $M_W = 80.45$ GeV (right curves). (a) Positive root, (b) negative root. There is no bound on M_2 to the right of the curves, since $M_1 \gtrsim M_Z$ for those regions.

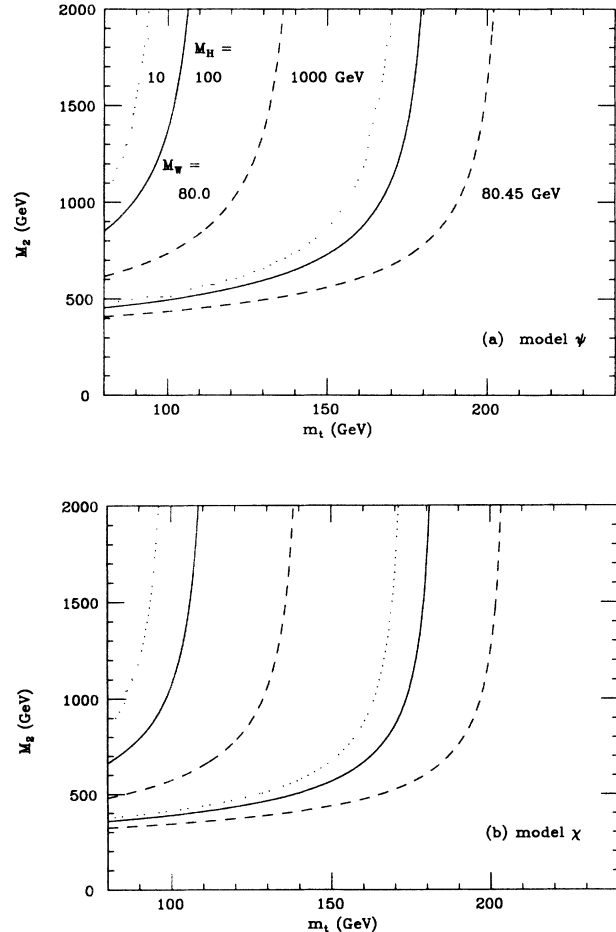


FIG. 10. Same as Fig. 9 but for (a) model ψ and (b) model χ . Note that the positive and negative roots are degenerate for these two models.

We are now ready to discuss the upper limits on M_2 in these various classes of models. Figures 9(a) and 9(b) show these limits as functions of m_t for $m_H = 10, 100,$ or 1000 GeV and for different W masses (corresponding to the CDF central value $\pm 1\sigma$) in the ER5M model η . Note that for the CDF 1σ lower limit ($M_W = 79.55$ GeV) there is no consistent solution for an upper limit on M_2 obtainable in this model for $m_t \geq 80$ GeV. [The reason for this is clearly demonstrated in Fig. 2(b).] Note also that the upper bound for the positive root of Eq. (3.11), shown in Fig. 9(a), is stronger than that obtained in the corresponding negative root case shown in Fig. 9(b). We see from these figures the general feature that as m_H increases the M_2 upper bound becomes stronger. In addition, as M_W increases the bound also becomes stronger for fixed m_H . The regions to the right of the curves, where the slopes get very large, correspond to $M_1 \geq M_Z$ for which there is no upper limit on M_2 . These regions are disallowed in this model. The value of m_t at which the slopes become large correspond to the m_t values in Fig. 2(b) for which the predicted M_Z range intersects the measured M_1 range. In the case of the positive root for model η a large fraction of the upper bounds found for the Z_2 mass are not far above the lower bounds obtained

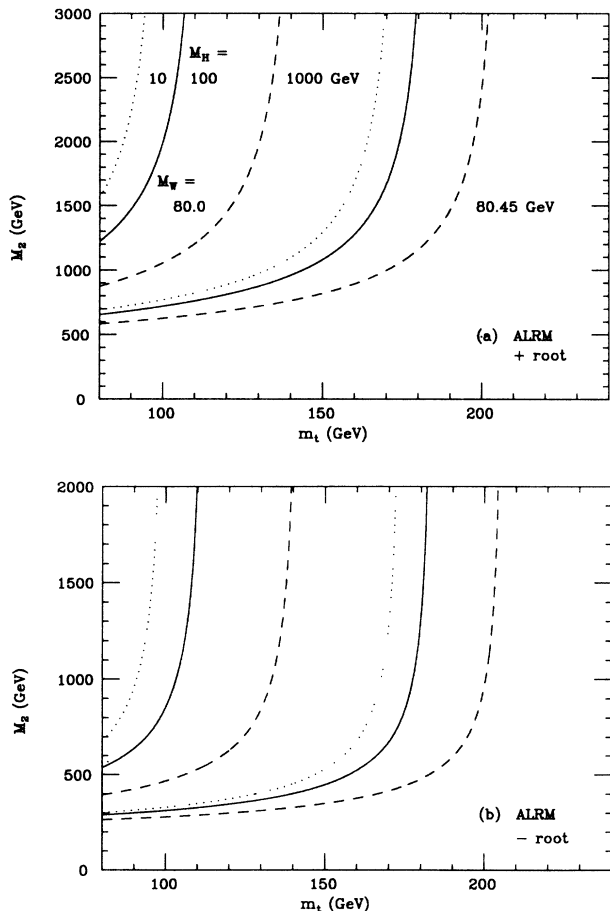


FIG. 11. Same as Fig. 9 but for the ALRM: (a) positive root; (b) negative root.

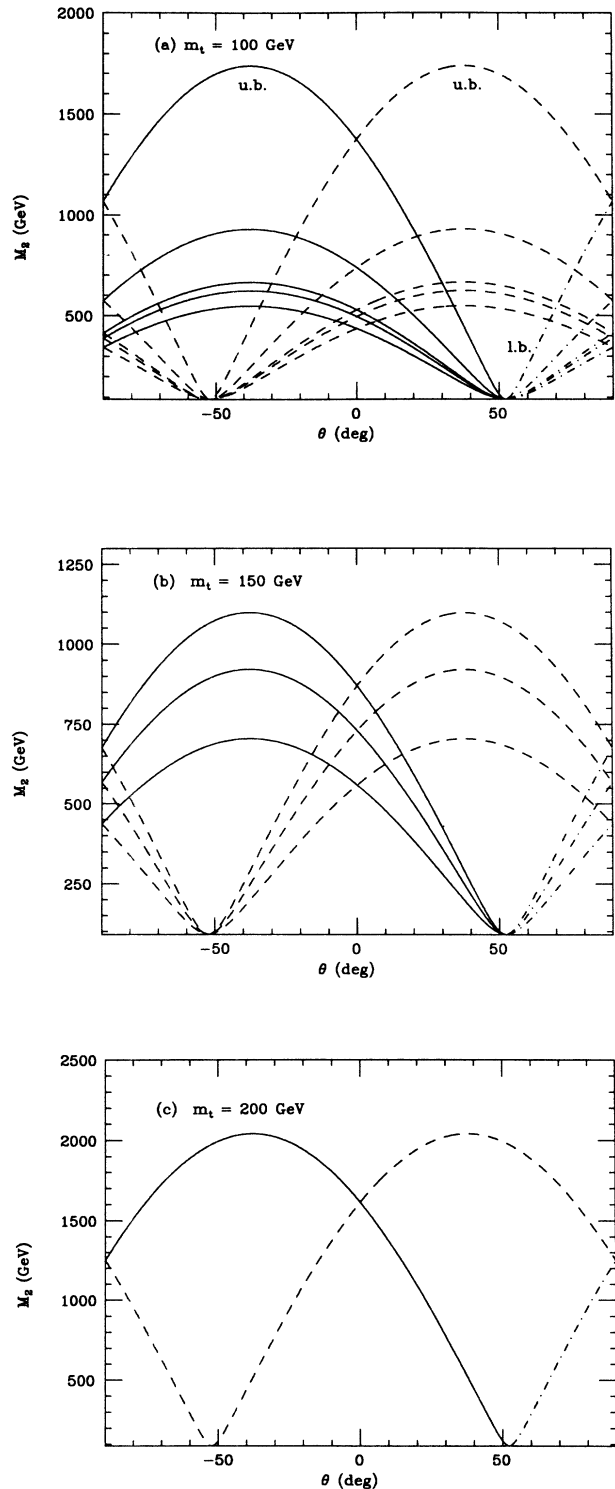


FIG. 12. Upper bounds on M_2 as a function of θ in the ER5M for both positive (solid) and negative (dashed) roots. (a) From top to bottom the curves correspond to $M_W = 80, m_H = 100$ GeV; $M_W = 80$ GeV, $m_H = 1$ TeV; $M_W = 80.45$ GeV, $m_H = 10$ GeV; $M_W = 80.45$ GeV, $m_H = 100$ GeV; and $M_W = 80.45$ GeV, $m_H = 1$ TeV, all with $m_t = 100$ GeV. (b) For $m_t = 150$ GeV and $M_W = 80.45$ GeV with $m_H = 10$ (upper), 100 (middle), and 1000 (lower) GeV. (c) for $m_t = 200$ GeV and $M_W = 80.45$ GeV with $m_H = 1$ TeV.

from the Fermilab Tevatron displayed in Fig. 8, but this is not the case for the bounds with the negative root.

Figure 10(a) shows the upper bounds on M_2 in model ψ where the positive and negative solutions of Eq. (3.11) are degenerate. These bounds show the same general behavior as those for model η (negative root). Similarly, Fig. 10(b) shows these bounds for model χ where again we have degenerate roots. Note that the upper bounds

obtained on M_2 for model χ are stronger than those (for a given set of m_t , m_H , and M_W values) obtained in Fig. 10(a) for model ψ .

Figures 11(a) and 11(b) show the corresponding upper limits on M_2 for the ALRM for the positive- and negative-root choices in Eq. (3.11). The LRM case yields an absolute prediction for M_2 (not an upper bound) which corresponds numerically to the positive-root solu-

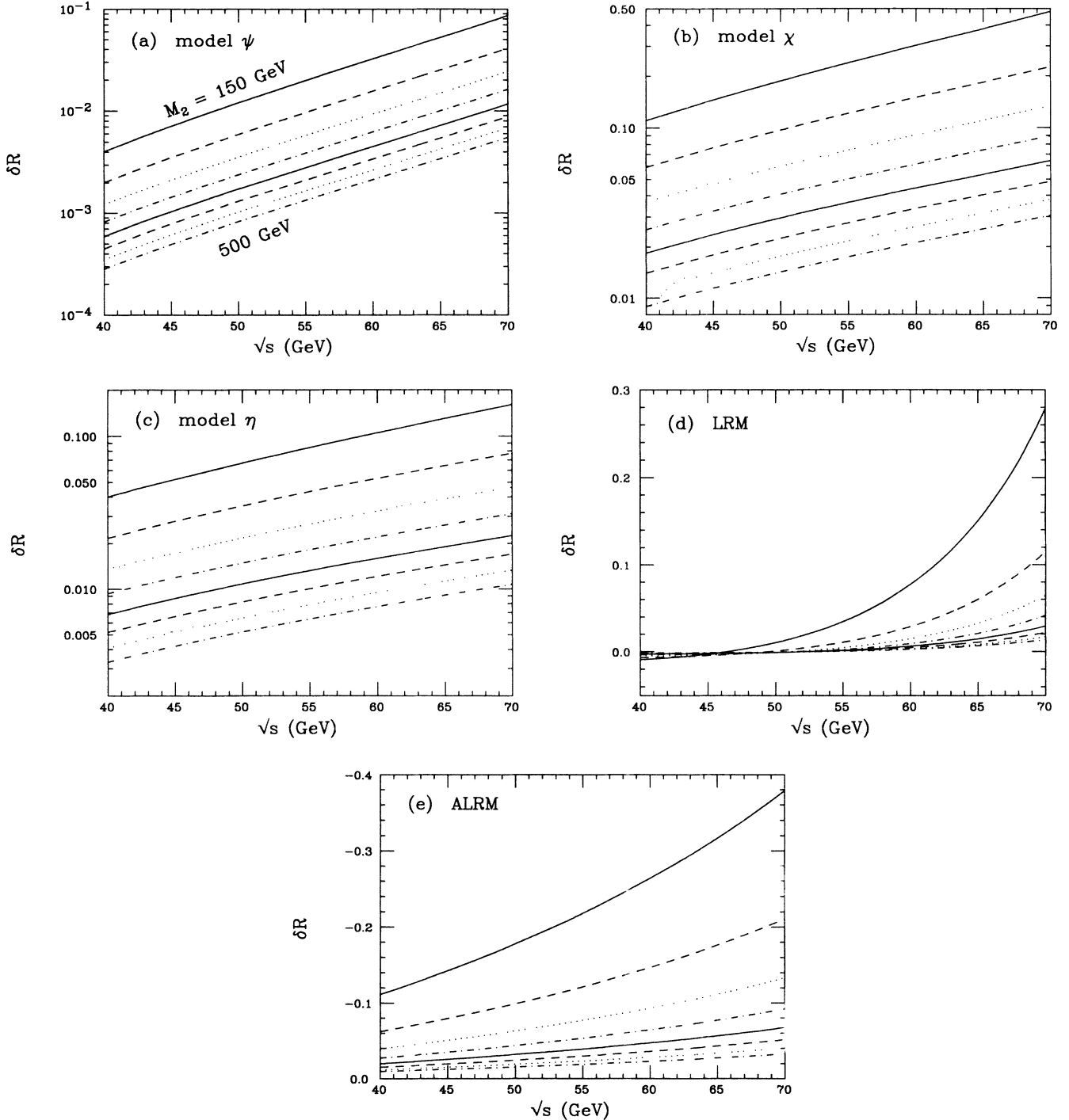


FIG. 13. Change in the R ratio (δR) as a function of \sqrt{s} for different Z' masses in the absence of Z - Z' mixing. The upper (lower) curve corresponds to $M_2 = 150$ (500) GeV with each subsequent curve corresponding to an increase in M_2 by 50 GeV. (a) Model ψ , (b) model χ , (c) model η , (d) the LRM, and (e) the ALRM.

tion in the case of the ALRM. While the ALRM positive root always yields an upper limit on M_2 which is ≥ 500 GeV, the negative root generally forces M_2 to be much lower, and a large region of the parameter space is already excluded when compared with the preliminary Fermilab Tevatron bounds.

How do the upper limits vary in general with the parameter θ in the ER5M? Figure 12(a) shows, for $m_t=100$ GeV, the positive- and negative-root solutions for these upper limits on M_2 as functions of θ for different choices of m_H and $M_W=80.0$ and 80.45 GeV. Note that no solutions are obtained for the CDF 1σ lower limit on M_W (i.e., $M_W=79.55$ GeV), corresponding to the results displayed in Fig. 2(b). Also shown, for $\theta \geq 52.24^\circ$, are the lower bounds on M_2 obtained by the same analysis. We again see that for fixed m_t the bounds on M_2 improve as either M_W or m_H increases. Figure 12(a) shows the degeneracy of the positive- and negative-root solutions for $\theta=0$ and -90° . It is also important to note that in the case of the ER5M with $\theta=90^\circ$ the limits we obtain on M_2 are actually *predictions* of M_2 since for $\theta=90^\circ$, $Q'_{\min}=Q'_{\max}$. Figures 12(b) and (c) show similar plots for $m_t=150$ and 200 GeV, where upper limits for M_2 only exist for the CDF 1σ upper value of M_W (i.e., $M_W=80.45$ GeV).

It is clear from this analysis that as the CDF determination of the W mass improves and the lower limits on M_2 from direct searches at the Fermilab Tevatron become stronger, very large regions of the presently allowed parameter space for the extended electroweak models considered here can be ruled out. It is expected that the CDF error on the W mass will be reduced to 0.30 GeV in the not too distant future.

IV. IMPLICATIONS FOR KEK TRISTAN ENERGIES

In this section we focus our discussion on the implications of new neutral gauge bosons at the KEK TRISTAN energy scale, i.e., $\sqrt{s} \approx 60$ GeV. The motivation for this investigation is the suggested $\approx 10\%$ increase observed at KEK TRISTAN in the value of

$$R = \frac{\sigma(e^+e^- \rightarrow \text{hadrons})}{\sigma_{\text{pt}}(e^+e^- \rightarrow \mu^+\mu^-)}, \quad (4.1)$$

with σ_{pt} being the usual QED point cross section ($=4\pi\alpha^2/3s$), for values of $\sqrt{s} \gtrsim 55$ GeV and the suggested decrease by $\approx 10\%$ in the value of

$$R_\mu = \frac{\sigma(e^+e^- \rightarrow \mu^+\mu^-)}{\sigma_{\text{pt}}(e^+e^- \rightarrow \mu^+\mu^-)} \quad (4.2)$$

in the same energy regime.⁴ It is unknown whether these two effects are related. It seems that the apparent rise in R is not due to the production of hadrons of a new flavor (b' , t , etc.) since these would modify not only R but also the jet distributions in this energy range in a manner which is not observed experimentally.⁴ Also, one might expect additional isolated leptons and/or photons from the subsequent heavy-quark decay and these are not observed. One possible explanation is that, instead of new particle production, there is new physics in either the s , t ,

or u channels which modify the production cross section without greatly modifying the jet distributions. Among the possibilities is the exchange of a Z' (in addition to the usual γ and Z) in the s channel.^{26,27} In our analysis we examine the influence of Z' exchange on both R and R_μ in the ER5M, ALRM, and LRM in the absence of Z - Z' mixing (i.e., $\phi=0$). We will show that for gauge-boson masses which satisfy the new preliminary Z' search limits from CDF, changes in R and R_μ by the amounts observed at KEK TRISTAN remain unexplainable within this scenario.

Let us first consider the case of hadron production. Figure 13 shows the change δR in R as a function of \sqrt{s} for various models with M_2 in the range $150 \leq M_2 \leq 500$ GeV. The model ψ case shown in Fig. 13(a) gives a very small change $\delta R \lesssim 0.04$ even for light M_2 's already excluded by CDF. For model χ [shown in Fig. 13(b)] the effect is somewhat larger, although for values of M_2 which survive the CDF preliminary search limits, one finds $\delta R \lesssim 0.05$. The cases of model η , the LRM, and the ALRM are shown in Figs. 13(c)–13(e), respectively. All of these models yield small $\delta R \lesssim 0.02$ values for large ($\gtrsim 300$ GeV) M_2 choices and in the ALRM δR is even

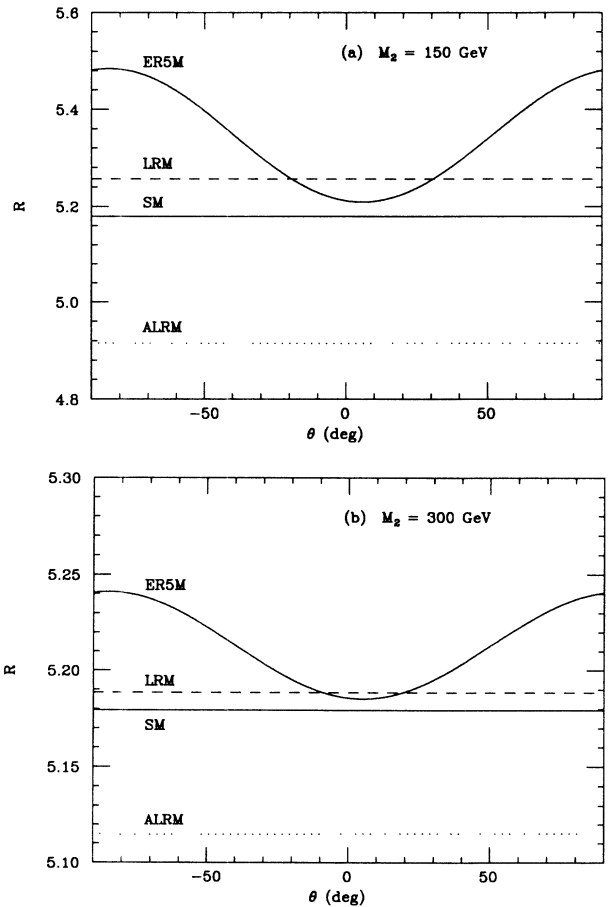


FIG. 14. The value of R at $\sqrt{s} = 60$ GeV for the SM (solid), ER5M as a function of θ (solid), LRM (dashed), and the ALRM (dotted). The curve showing the greatest (least) deviation from the SM corresponds to (a) $M_{Z'}=150$ GeV and (b) $M_{Z'}=300$ GeV.

negative. Is it possible for some other value of θ that δR can be large enough to accommodate the KEK TRISTAN R ratio and yet M_2 still satisfy the CDF limits? Figures 14(a) and 14(b) show, for $\sqrt{s} = 60$ GeV, R as a function of θ in the ER5M together with the SM, LRM, and ALRM predictions with $M_2 = 150$ and 300 GeV, respectively. While large δR 's are obtainable for

$M_2 = 150$ GeV, taking $M_2 = 300$ GeV to satisfy the CDF bounds reduces the maximal δR in the ER5M to ≈ 0.06 . Note that the values of R in the ER5M are left invariant by shifting θ by 180° , i.e., by mapping $\theta \rightarrow \theta + 180^\circ$. Clearly there does not exist a Z' in any of these models which can simultaneously satisfy the CDF constraints and increase R by the desired amount.

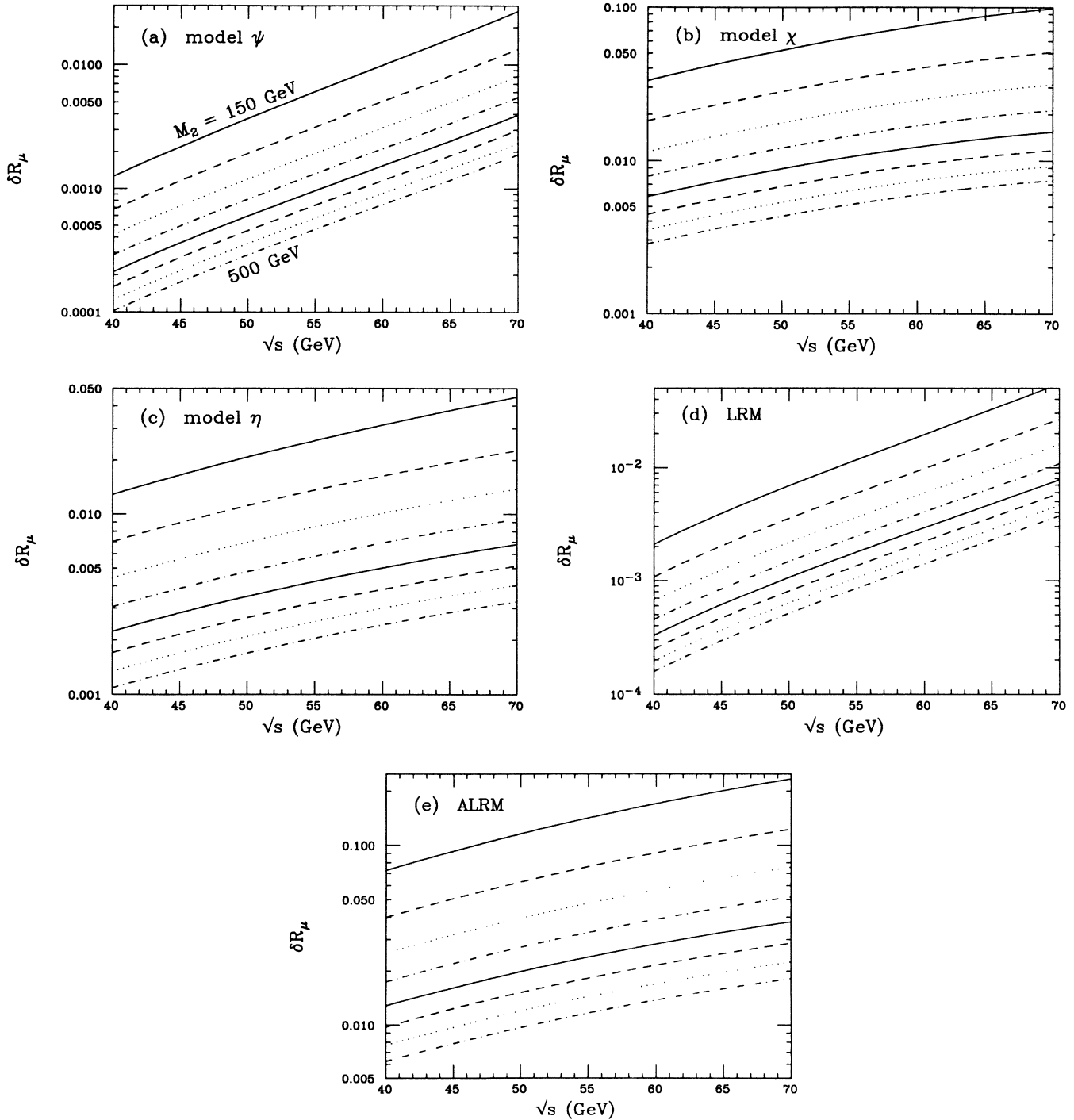


FIG. 15. Change in the ratio R_μ (δR_μ) as a function of \sqrt{s} for the same models and Z' masses as shown in Fig. 13: (a) model ψ , (b) model χ , (c) model η , (d) the LRM, and (e) the ALRM.

Can a new Z' explain the observed decrease in R_μ at KEK TRISTAN? Figure 15 shows δR_μ (the change in R_μ) due to Z' exchange in various models as a function of \sqrt{s} for different values of M_2 . Since δR_μ is found to be positive for model ψ [Fig. 15(a)] and the LRM [Fig. 15(d)] these can be immediately excluded from further consideration. We now ask whether the other models can accommodate a $\delta R_\mu \simeq -0.1$ while satisfying the CDF preliminary search limits. Unfortunately, for $M_2 \gtrsim 300$ GeV, all of these models predict a $|\delta R_\mu| \lesssim 0.03$ with the ALRM [in Fig. 15(e)] yielding the largest value. Figure 16 provides further proof that producing a large $|\delta R_\mu|$ is impossible in any of these models for M_2 values $\gtrsim 300$ GeV. Figure 16(a) shows that, even for $M_2 = 150$ GeV, only the ALRM can produce a small enough value of R_μ to be consistent with the KEK TRISTAN data; for $M_2 = 300$ GeV, shown in Fig. 16(b), it is clear that no model produces a sufficiently large $|\delta R_\mu|$.

It is clear from this analysis that none of the new gauge bosons from any of the above models can explain the

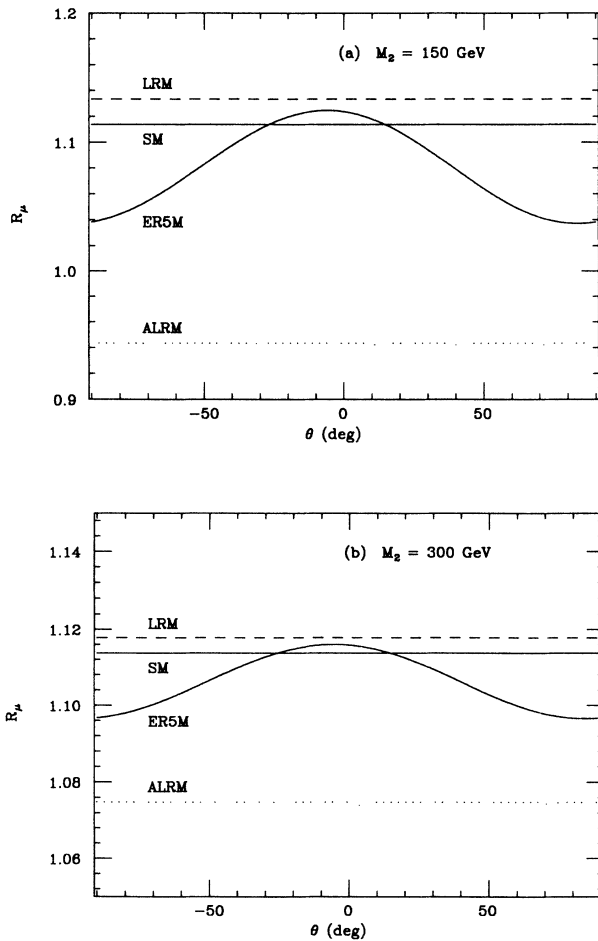


FIG. 16. Same as Figs. 14(a) and 14(b) but for R_μ for the SM (solid), ER5M as a function of θ (solid), LRM (dashed), and the ALRM (dotted).

KEK TRISTAN data on R and R_μ , and simultaneously satisfy the preliminary CDF limits on their mass.

How do these results change if we give up the assumption that $\phi = 0$? A short analysis shows that while δR and δR_μ are somewhat sensitive to nonzero values of ϕ , the values of δR and δR_μ obtained for $M_2 = 300$ GeV are still too small to account for the effects observed at KEK TRISTAN.

V. SUMMARY AND CONCLUSIONS

In this paper we have analyzed the implications of recent measurements of W and Z gauge-boson properties and e^+e^- annihilation cross sections at the SLC, LEP, Fermilab Tevatron, and KEK TRISTAN. We have made a detailed comparison of the SM predictions, including radiative corrections, with the masses of the Z and W gauge bosons and the Z decay width. We found that experiment and theory are in good agreement, but some room still remains for deviation from SM predictions and further improvements in the data are necessary before extended electroweak gauge groups can be excluded. We have analyzed the effects of Z - Z' mixing on the values of Z width, leptonic branching fraction, and resonance height at e^+e^- colliders for a number of different extended electroweak gauge models. We found that the Z peak height is very sensitive to such mixing even for modest values of the Z - Z' mixing angle ϕ . Using the existing data on M_W and M_Z , we placed model-dependent *upper* limits on the mass of the second neutral gauge boson and compared these to the model-dependent *lower* bounds on this mass from the preliminary CDF Z' search limits. For example, in model $\psi(\chi)$, Figs. 12(a) and (12b) show that with $M_W = 80.45$ GeV and $m_t \lesssim 150$ GeV the upper bounds on M_2 are $\lesssim 750$ GeV ($\lesssim 650$ GeV) while the direct searches at CDF yield $M_2 \gtrsim 300$ GeV. We analyzed the possible influence of new gauge bosons on the hadron and $\mu^+\mu^-$ production cross sections at KEK TRISTAN energies. We found that, for the models examined, the increase in R and decrease in R_μ observed at KEK TRISTAN could not be explained for values of the gauge-boson masses which satisfy the preliminary CDF search limits on an extra Z boson.

Further improvements in the data on gauge-boson properties (which should become available in the near future) will either show indication for or rule out large regions of parameter space of extended electroweak models.

ACKNOWLEDGMENTS

We thank Duncan Morris for discussions and use of his programs for calculating radiative corrections. One of us (T.G.R.) would like to thank the Phenomenology Institute at the University of Wisconsin-Madison for its hospitality and use of its facilities. This research was supported in part by the University of Wisconsin Research Committee with funds granted by the Wisconsin Alumni Research Foundation, and in part by the U.S. Department of Energy under Contracts Nos. DE-AC02-76ER00881 and W-7405-Eng-82.

- ¹UA2 Collaboration, R. Ansari *et al.*, Phys. Lett. B **186**, 440 (1987); UA1 Collaboration, G. Arnison *et al.*, Phys. Lett. **166B**, 484 (1986); P. Tipton, talk presented at Collider Phenomenology Workshop, Argonne National Laboratory, 1989 (unpublished).
- ²ALEPH Collaboration, S.-L. Wu, DELPHI Collaboration, A. Firestone, L3 Collaboration, J. Branson, and OPAL Collaboration, W. Gary, talks given at the Annual Rice University Meeting of the Division of Particles and Fields of the APS, Houston, Texas, 1990 (unpublished).
- ³S. Errede, talk presented at the Meeting of the Division of Particles and Fields of the APS (Ref. 2); CDF Collaboration, Phys. Rev. Lett. **63**, 720 (1989).
- ⁴A. Maki, in *Proceedings of the 14th International Symposium on Lepton and Photon Interactions*, Stanford, California, 1989, edited by M. Riordan (World Scientific, Singapore, 1990); see VENUS Collaboration, K. Abe *et al.*, Phys. Rev. D **39**, 3524 (1989); AMY Collaboration, T. Mori *et al.*, Phys. Lett. B **218**, 499 (1989).
- ⁵A. Sirlin, Phys. Rev. D **22**, 971 (1980); W. J. Marciano and A. Sirlin, *ibid.* **22**, 2695 (1980); **29**, 945 (1984); **31**, 213(E) (1985).
- ⁶F. Halzen and D. Morris, Phys. Lett. B **237**, 107 (1990); D. Morris (private communication).
- ⁷W. Hollik, Report No. DESY 88/188, 1988 (unpublished); Report No. CERN-TH5426/89, 1989 (unpublished); see also M. Consoli and W. Hollik, CERN Yellow Report No. 89-08, 1989, Vol. I, p. 7, (unpublished); G. Burgers and F. Jegerlehner, *ibid.*, p. 55.
- ⁸A. Djouadi and C. Verzegnassi, Phys. Lett. B **195**, 265 (1987); A. Djouadi, Nuovo Cimento **100A**, 357 (1988).
- ⁹J. J. van der Bij and F. Hoogeveen, Nucl. Phys. **B283**, 471 (1987).
- ¹⁰See, for example, J. H. Kuhn and P. M. Zerwas, CERN Yellow Report No. 89-08, 1989, Vol. I, p. 267, (unpublished); Z. Kunst and P. Nason, *ibid.*, p. 373.
- ¹¹T. Hansl-Kozanecka, talk given at the SLD Physics Workshop, Kirkwood, California, 1989 (unpublished).
- ¹²B. A. Kniehl, J. H. Kuhn, and R. G. Stuart, Phys. Lett. B **214**, 621 (1988); B. A. Kniehl *et al.*, *ibid.* **209**, 337 (1988).
- ¹³Particle Data Group, G. Yost *et al.*, Phys. Lett. B **239**, 1 (1990).
- ¹⁴CDF Collaboration, F. Abe *et al.*, Phys. Rev. Lett. **64**, 152 (1990).
- ¹⁵J. Ellis and G. Fogli, Phys. Lett. B **231**, 189 (1989).
- ¹⁶U. Amaldi *et al.*, Phys. Rev. D **36**, 1385 (1987); G. Costa *et al.*, Nucl. Phys. **297**, 244 (1988); J. Ellis and G. Fogli, Phys. Lett. B **213**, 526 (1988); **231**, 189 (1989); D. Haidt, in *Weak Interactions and Neutrinos*, proceedings of the 12th International Workshop, Ginosar, Israel, 1989, edited by P. Singer and B. Gad Eilam [Nucl. Phys. B (Proc. Suppl.) **13** (1989)].
- ¹⁷For a recent review, see J. L. Hewett and T. G. Rizzo, Phys. Rep. **183**, 193 (1989).
- ¹⁸E. Ma, Phys. Rev. D **36**, 274 (1987); Mod. Phys. Lett. A **3**, 319 (1988); K. S. Babu, X.-G. He, and E. Ma, Phys. Rev. D **36**, 878 (1987); E. Ma and D. Ng, *ibid.* **39**, 1986 (1989).
- ¹⁹For original references and a general survey of the left-right-symmetric model, see R. N. Mohapatra, *Unification and Supersymmetry* (Springer, New York, 1986).
- ²⁰P. Langacker and S. Uma Sankar, University of Pennsylvania report, 1989 (unpublished).
- ²¹T. G. Rizzo, Mod. Phys. Lett. A **5**, 115 (1990); Phys. Rev. D **40**, 3035 (1989).
- ²²L. Nodulman, talk presented at the International Europhysics Conference on High Energy Physics, Madrid, Spain, 1989 (unpublished).
- ²³D. Duke and J. Owens, Phys. Rev. D **30**, 49 (1984).
- ²⁴E. Eichten *et al.*, Rev. Mod. Phys. **56**, 579 (1984).
- ²⁵J. Abad and B. Humpert, Phys. Lett. **78B**, 627 (1978); G. Altarelli, R. K. Ellis, and G. Martinelli, Nucl. Phys. **B157**, 461 (1979); J. Kubar-André and F. Paige, Phys. Rev. D **19**, 221 (1979); V. Barger and R. J. N. Phillips, *Collider Physics* (Frontiers in Physics, Vol. 71) (Addison-Wesley, Reading, MA, 1987).
- ²⁶K. Hagiwara, R. Najima, M. Sakuda, and N. Terunuma, University of Durham report, 1989 (unpublished); A. Pankov and C. Verzegnassi, Phys. Lett. B **233**, 259 (1989).
- ²⁷Another possibility is the exchange of a leptoquark in the u channel. For a discussion of this case, see D. Zeppenfeld, talk given at the KEK Topical Conference on e^+e^- Collision Physics 89, Tsukuba, Japan, 1989 (unpublished).